Supporting Information

Hybrid Nanogels by Direct Mixing of Chitosan, Tannic Acid and Magnetite Nanoparticles: Processes Involved in Their Formation and Potential Catalytic Properties

Santiago Marzini Irranca[a,c†], Sergio D. García Schejtman[a,c†*], Anabella P. Rosso[a,d], Eduardo A. Coronado[b,d*] and Marisa Martinelli[a,c*]

[a] Universidad Nacional de Córdoba. Facultad de Ciencias Químicas. Departamento de Química Orgánica. Materiales Poliméricos, Híbridos y Nanoarquitectónicos (LaMaP). Córdoba, Argentina

[b] Universidad Nacional de Córdoba. Facultad de Ciencias Químicas. Departamento de Fisicoquímica. Plasmónica Molecular. Bio(nanoplasmónica). Espectroscopías ultrasensibles. Córdoba, Argentina

[c] Instituto de Investigación y Desarrollo en Ingeniería de Procesos y Química Aplicada (IPQA). CONICET. Córdoba, Argentina

[d] Instituto de Investigaciones en Físico-Química de Córdoba (INFIQC). CONICET. Córdoba, Argentina

*Corresponding authors:

- coronado@fcq.unc.edu.ar

- marisa.martinelli@unc.edu.ar

- dgarcia@unc.edu.ar

† These authors contributed equally to this work.

FT-IR characterisation of TA and OTA:

The FT-IR spectrum of pure TA exhibit different characteristic bands: a broad band at 3315 cm^{-1} corresponding to the stretching vibration of O-H groups in the polyphenol molecule, an intense band at 1695 cm^{-1} assigned to the C=O stretching modes of ester groups, a band at 1444 cm^{-1} attributed to the bending O-H vibration of the pyrogallol molecule; and the band at 1185 cm^{-1} due to the stretching vibration of C-OH bond of the -OH groups in the benzene rings. The OTA spectrum presents the same vibrational modes but the 3315, 1444 and 1185 cm^{-1} bands have lower relative intensity than that observed in the TA spectrum, evidencing the oxidation of the phenolic -OH groups. Another proof of oxidation is the appearance of a signal at 1675 cm^{-1} characteristic of the vibration of C=O groups of o-quinones, and the shoulder in this signal at 1695 cm^{-1} can be attributed to the vibration of C=O groups, corresponding to the TA ester groups that do not undergo modification.

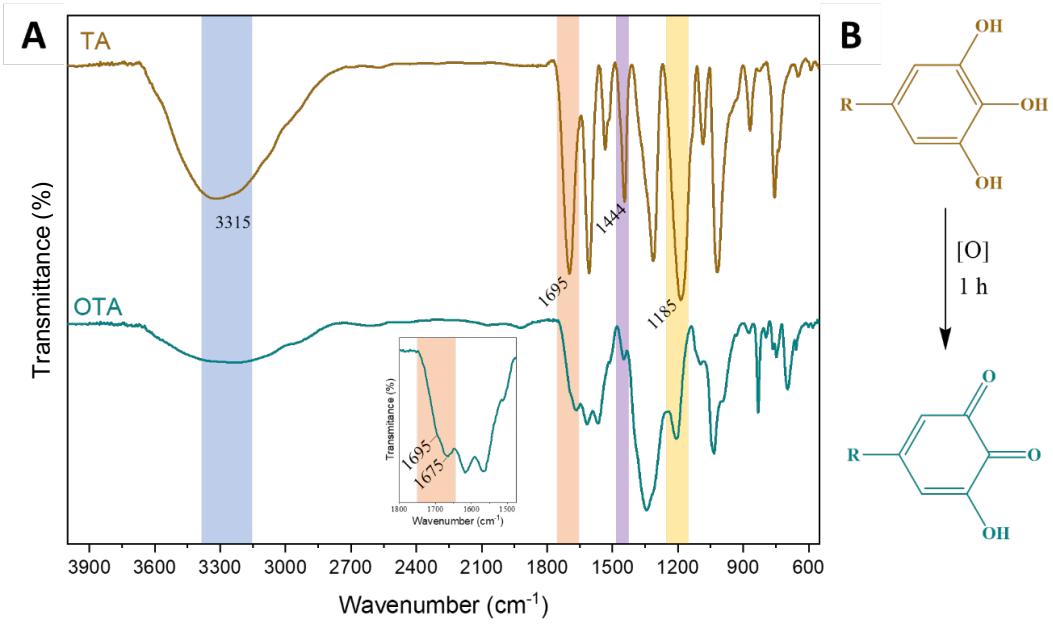

Fig. S1. (A) FT-IR spectra of TA and TAox, with a magnification of 1800 – 1500 cm^{-1} for the TAox spectrum. **(B)** TA oxidation reaction.

XPS of MNPs and MNPs@OTA

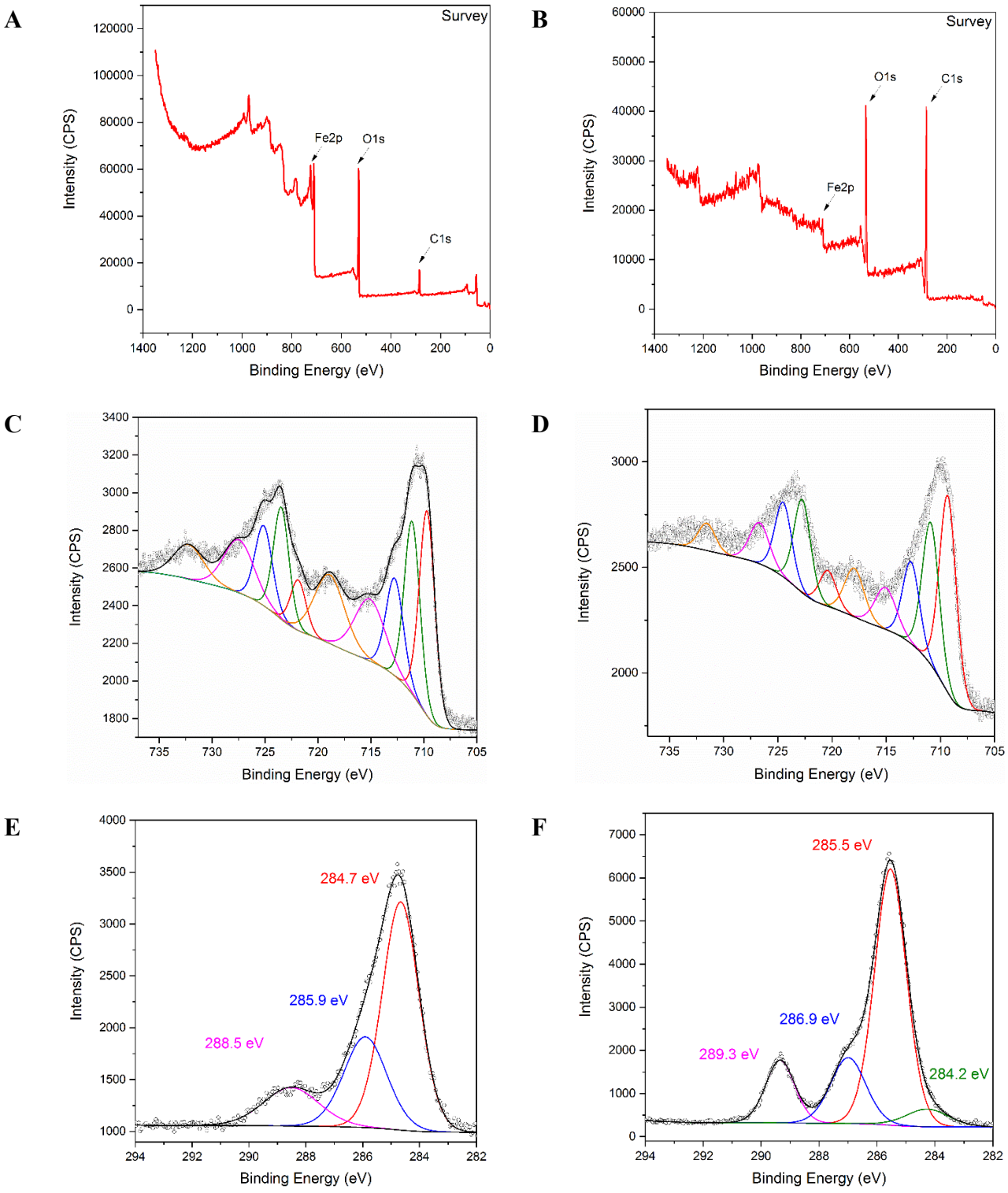

Fig. S2. XPS survey of (**A**) MNPs and (**B**) MNPs@OTA. Fe2p spectra of (**C**) MNPs and (**D**) MNPs@OTA. C1s spectra of (**E**) MNPs and (**F**) MNPs@OTA.

Table S1. Results of the curve fitting analysis of XPS spectra of MNPs sample.

Component	BE (eV)	Assignment
C1s	284.7	Aliphatic carbon: C-H; C-C
	285.9	C-O-C
	288.5	Carboxylates
O1s	529.9	Fe-O
	531.4	O-H
	532.6	Organic impurities
Fe2p	709.7	Fe(II)
	711.1	Fe(III) oct., Fe_2O_3, FeOOH
	712.8	Fe(III) tetr. + multip.
	715.3	Fe(II) sat.
	719.0	Fe(III) sat.

Table S1. Results of the curve fitting analysis of XPS spectra of MNPs@OTA sample.

Component	BE (eV)	Assignment
C1s	284.2	C=C (Aromatic ring)
	285.5	C-H and C-C
	286.9	C-O-C
	289.3	Carboxylates
O1s	529.9	Fe-O
	532.3	Organic C-O
	533.7	Organic C=O
Fe2p	709.4	Fe(II)
	711.0	Fe(III) oct., Fe_2O_3, FeOOH
	712.7	Fe(III) tetr. + multip.
	715.1	Fe(II) sat.
	718.0	Fe(III) sat.

Thermogravimetric analysis of MNPs and MNPs@OTA

The TGA curves for MNPs and MNPs@OTA are shown in Fig. S3. The TGA curve of MNPs shows an initial mass loss of around 2% at 286 °C (Fig. S3A), mostly related to the desorption of adsorbed water and some dehydration products generated by ambient moisture.[1,2] In the case of MNPs@OTA (Fig. S3B), a weight loss with a centred peak at 286 °C is observed, indicating the loss due to the TA moiety of MNPs. Considering that up to 600°C, a weight gain in MNPs@OTA TGA curve is observed due to oxidation processes of magnetite, [1] the comparison of TGA curves was performed to avoid this. The mass loss attributed to the TA functionalities was considered as 4.2%.

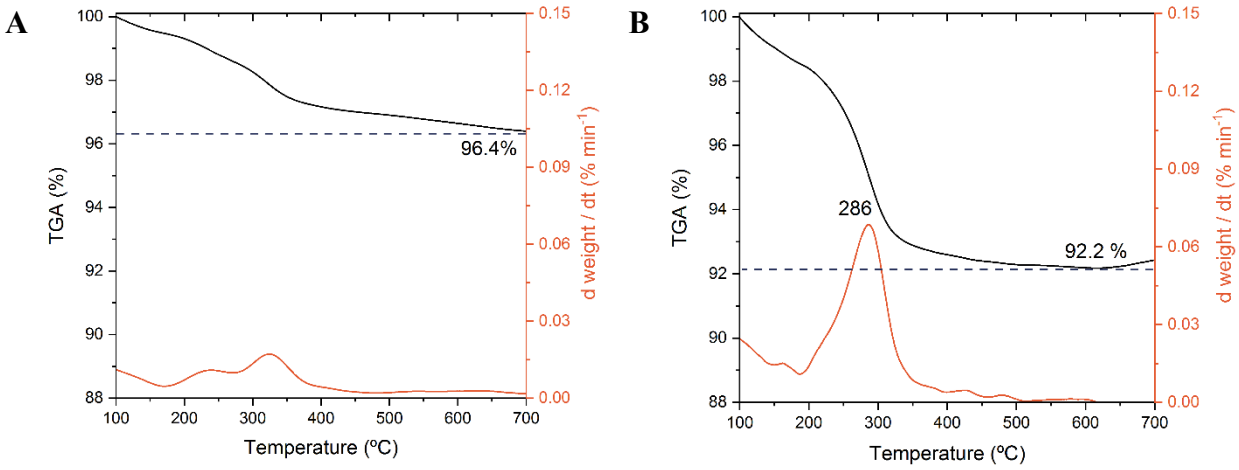

Fig. S3. TGA and DTG curves for (**A**) MNPs and (**B**) MNPs@OTA.

Assuming that the TA forms a close-packed monolayer on the nanoparticles, the total weight loss due to the loss of organic molecule can be calculated theoretically by using the equation (eq. S1):[2,3]

$$W_{loss} = \frac{100\left[\left(\frac{\pi\, d_{MNPs}^2}{a}\right)\frac{MW_{TA}}{N_A}\right]}{\frac{1}{6}\,\pi\, d_{MNPs}^3\,\rho_{MNPs} + \left(\frac{\pi\, d_{MNPs}^2}{a}\right)\frac{MW_{TA}}{N_A}} \quad \text{(S1)},$$

were d is the mean diameter of MNPs, a is the tabulated projected area of the TA (7.78 nm^2), MW is the molecular weight of TA, N_A is the Avogadro's number and ρ is the MNPs density (5.2 g mL^{-1}). The calculated value for the weight loss is found to be 3.5%. Since the experimental weight loss was 4.2% (see Fig. S3), the differences between the two values could be attributed to the polydispersity of particle diameter, or even to the steric hindrance due to a volumetric molecular such as TA. Furthermore, it is important to consider that the TA could induce auto-polymerization at oxidative conditions. For that, the high weight loss value could be understood as a functionalisation of TA with a certain amount of its dimers or oligomers in the nanoparticle surface.

Obtention of Nanocatalytic Nanogels

For the SEM-EDS results, we took specific images of different nanogels with larger sizes or aggregates, due to (i) the limitations of the piece of equipment, and (ii) to obtain images with better resolution.

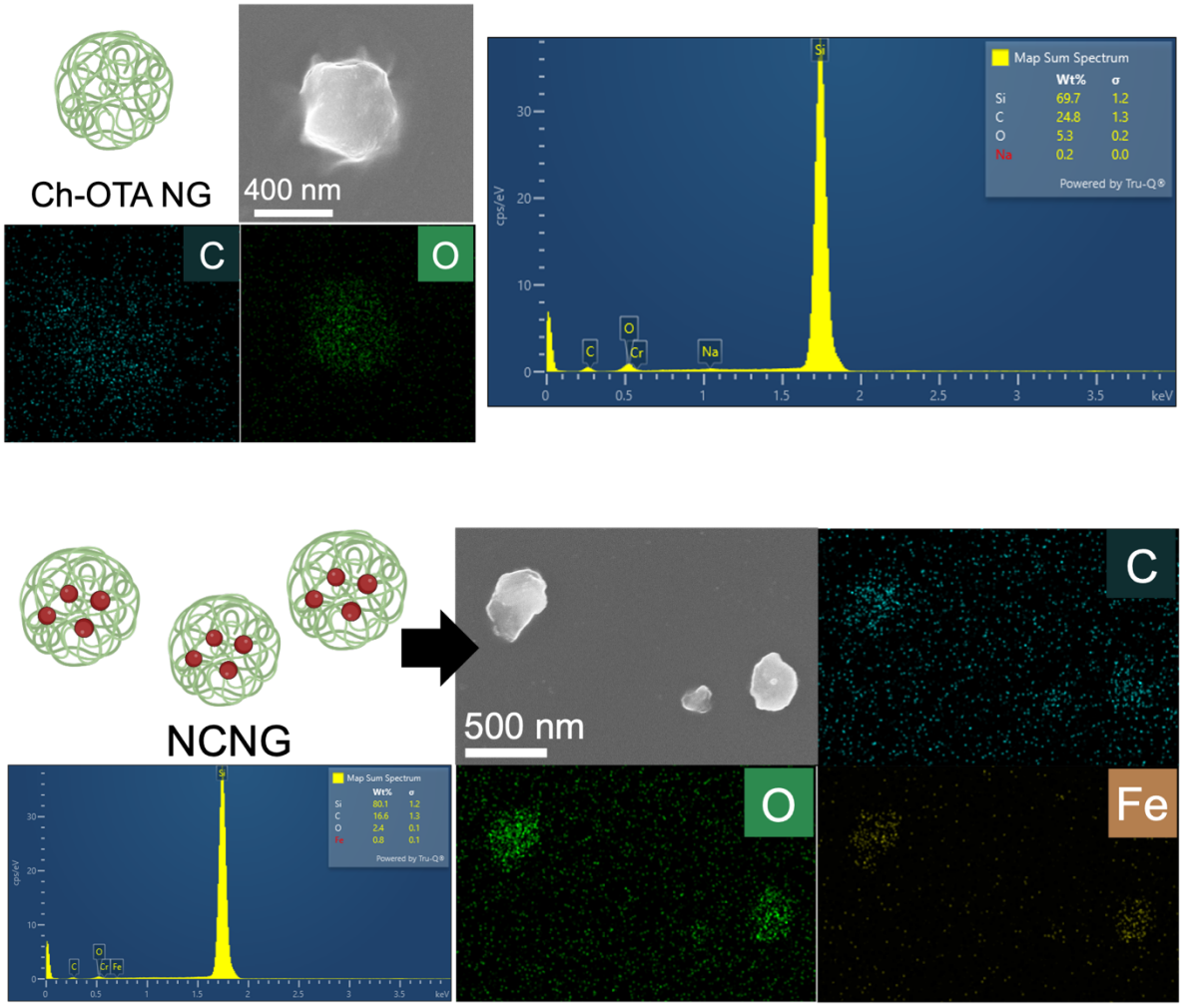

Fig. S4. SEM-EDS images for different obtained nanogels.

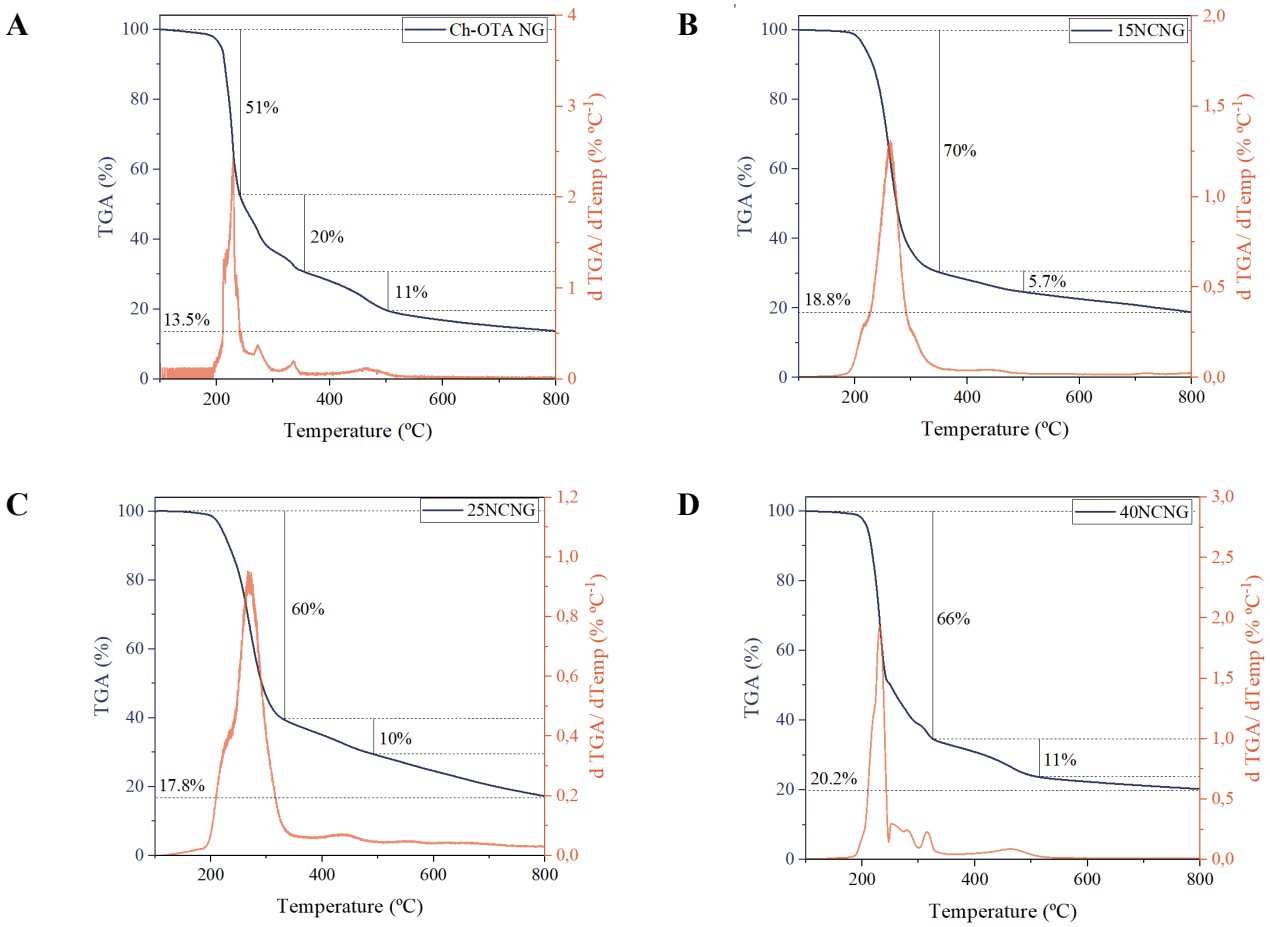

Fig. S5. Thermogravimetric analysis for the prepared nanogels.

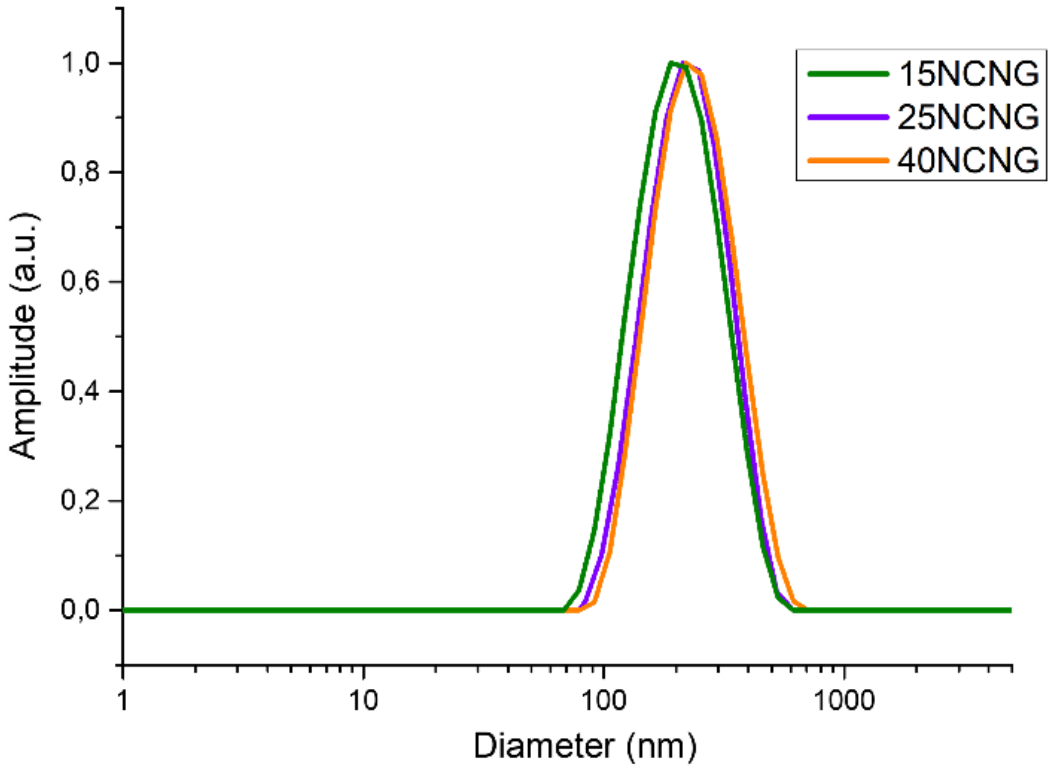

Fig. S6. Size distribution for 15NCNG, 25NCNG and 40NCNG determined by DLS measurements. Each measurement has been performed in triplicate and repeating the same measurement every week over a month.

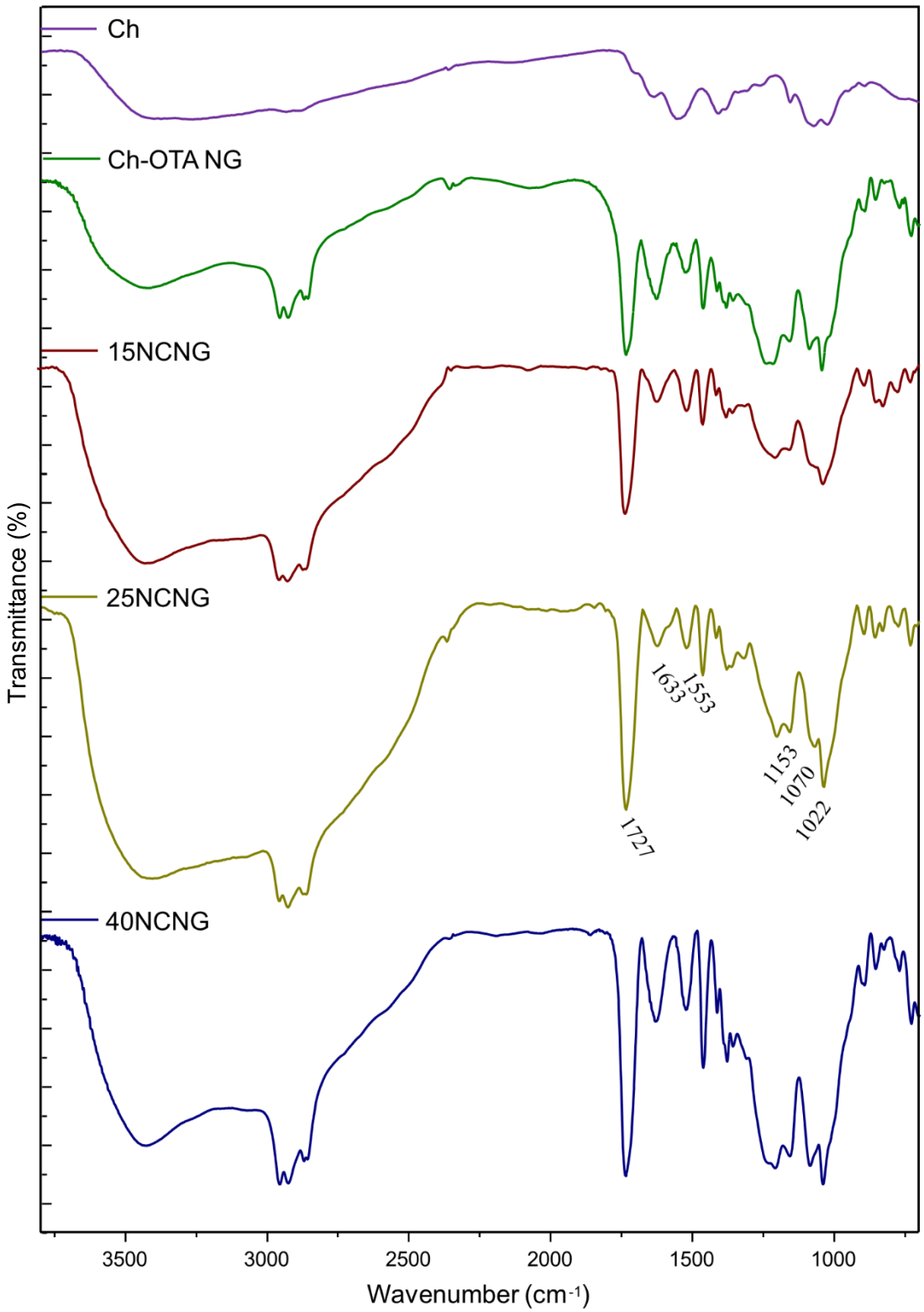

Fig. S7. FT-IR spectra of pure Ch, Ch-OTA NG, 15NCNG, 25NCNG and 40NCNG.

References:

(1) Iyengar, S. J.; Joy, M.; Ghosh, C. K.; Dey, S.; Kotnala, R. K.; Ghosh, S. Magnetic, X-Ray and Mössbauer Studies on Magnetite/Maghemite Core–Shell Nanostructures Fabricated through an Aqueous Route. *RSC Adv* **2014**, *4* (110), 64919–64929. https://doi.org/10.1039/C4RA11283K.

(2) Selzer, S. M.; Vico, R. v.; Ferreyra, N. F. Immobilization of Concanavalin A on Iron Oxide Magnetic Nanoparticles. Effect of Bovine Serum Albumin in the Recognition Interactions of the Lectin. *Surfaces and Interfaces* **2022**, *30*. https://doi.org/10.1016/j.surfin.2022.101908.

(3) Gnanaprakash, G.; Ayyappan, S.; Jayakumar, T.; Philip, J.; Raj, B. Magnetic Nanoparticles with Enhanced γ-Fe2O3 to α-Fe2O3 Phase Transition Temperature. *Nanotechnology* **2006**, *17* (23), 5851–5857. https://doi.org/10.1088/0957-4484/17/23/023.